Title

Bidirectional Contrast agent leakage correction of dynamic susceptibility contrast (DSC)-MRI improves cerebral blood volume estimation and survival prediction in recurrent glioblastoma treated with bevacizumab

Journal

Journal of Magnetic Resonance Imaging, 44(5)

ISSN

1053-1807

Authors

Leu, Kevin
Boxerman, Jerrold L
Lai, Albert
et al.

Publication Date

2016-11-01

DOI

10.1002/jmri.25227

Peer reviewed

Bidirectional Contrast Agent Leakage Correction of Dynamic Susceptibility Contrast (DSC)-MRI Improves Cerebral Blood Volume Estimation and Survival Prediction in Recurrent Glioblastoma Treated With Bevacizumab

Kevin Leu AB,[1,2,3] Jerrold L. Boxerman MD,PhD,[6] Albert Lai MD,PhD,[4,7] Phioanh L. Nghiemphu, MD,[4,7] Whitney B. Pope MD,PhD,[2] Timothy F. Cloughesy MD,[4,7] and Benjamin M. Ellingson, PhD[1,2,3,4,5]*

Purpose: To evaluate a leakage correction algorithm for T_1 and T_2^* artifacts arising from contrast agent extravasation in dynamic susceptibility contrast magnetic resonance imaging (DSC-MRI) that accounts for bidirectional contrast agent flux and compare relative cerebral blood volume (CBV) estimates and overall survival (OS) stratification from this model to those made with the unidirectional and uncorrected models in patients with recurrent glioblastoma (GBM).
Materials and Methods: We determined median rCBV within contrast-enhancing tumor before and after bevacizumab treatment in patients (75 scans on 1.5T, 19 scans on 3.0T) with recurrent GBM without leakage correction and with application of the unidirectional and bidirectional leakage correction algorithms to determine whether rCBV stratifies OS.
Results: Decreased post-bevacizumab rCBV from baseline using the bidirectional leakage correction algorithm significantly correlated with longer OS (Cox, $P = 0.01$), whereas rCBV change using the unidirectional model ($P = 0.43$) or the uncorrected rCBV values ($P = 0.28$) did not. Estimates of rCBV computed with the two leakage correction algorithms differed on average by 14.9%.
Conclusion: Accounting for T_1 and T_2^* leakage contamination in DSC-MRI using a two-compartment, bidirectional rather than unidirectional exchange model might improve post-bevacizumab survival stratification in patients with recurrent GBM.
J. MAGN. RESON. IMAGING 2016;00:000–000.

Glioblastoma (GBM) is the most common primary malignant brain tumor in adults, with 10,000 new cases arising per year in the United States.[1] Median overall survival is ~12–15 months with surgery and radiochemotherapy.[2,3] GBMs are among the most angiogenic of malignant tumors,[4] with hallmark features including cooption of existing vasculature and induction of new blood vessel growth via vascular endothelial growth factor (VEGF). Currently, bevacizumab, a humanized monoclonal antibody specifically targeting VEGF, is US Food and

View this article online at wileyonlinelibrary.com. DOI: 10.1002/jmri.25227

Received Jan 12, 2016, Accepted for publication Feb 24, 2016.

*Address reprint requests to: B.M.E., Director, UCLA Brain Tumor Imaging Laboratory (BTIL), Associate Professor of Radiology, Biomedical Physics, Bioengineering, and Psychiatry, Departments of Radiological Sciences and Psychiatry, David Geffen School of Medicine, University of California, Los Angeles, 924 Westwood Blvd., Suite 615, Los Angeles, CA 90024. E-mail: bellingson@mednet.ucla.edu

From the [1]UCLA Brain Tumor Imaging Laboratory (BTIL), Center for Computer Vision and Imaging Biomarkers, University of California, Los Angeles, Los Angeles, California, USA; [2]Department of Radiological Sciences, David Geffen School of Medicine, University of California, Los Angeles, Los Angeles, California, USA; [3]Department of Bioengineering, Henry Samueli School of Engineering and Applied Science, University of California, Los Angeles, Los Angeles, California, USA; [4]UCLA Neuro-Oncology Program, University of California, Los Angeles, Los Angeles, California, USA; [5]Department of Biomedical Physics, David Geffen School of Medicine, University of California, Los Angeles, Los Angeles, California, USA; [6]Department of Diagnostic Imaging, Rhode Island Hospital and Alpert Medical School of Brown University, Providence, Rhode Island, USA; and [7]Department of Neurology, David Geffen School of Medicine, University of California, Los Angeles, Los Angeles, California, USA.

Drug Administration (FDA)-approved for the treatment of recurrent GBM.

Because antiangiogenic therapy may decrease the contrast-enhancing lesion volume on conventional T_1-weighted postcontrast MRI, despite the absence of cytotoxic effect,[5,6] there is growing interest in using perfusion magnetic resonance imaging (MRI) to evaluate changes in blood volume as a noninvasive method of assessing the efficacy of anti-VEGF therapies.[7–9] In particular, relative cerebral blood volume (rCBV), a parameter computed by integrating the dynamic susceptibility contrast (DSC)-MRI relaxivity–time curve following the principles of indicator dilution theory,[10] is the most common MRI-based perfusion measurement used in neurooncology.[11] It is generally accepted that rCBV is elevated in tumors and decreases with successful chemoradiation-induced reduction in tumor-area blood vessels.

Since DSC-MRI is based on the indicator dilution theory,[10,12] the main assumption is that the injected contrast agent remains solely in the intravascular compartment. However, contrast agent extravasates into the extravascular, extracellular space (EES) during dynamic imaging of high-grade gliomas characterized by blood–brain barrier disruption,[13] causing artifactual T_1 or T_2^* effects that increase and decrease, respectively, the measured relaxivity–time curve, thereby impacting computed rCBV.[14] A popular leakage correction algorithm models unidirectional flux of contrast agent from the intravascular to the EES.[13,15] It operates by modeling the relaxivity–time curve from the DSC-MRI measurements as the sum of two terms: one derived from the average relaxivity in nonenhancing tissues, where contrast agent does not leak, and the other that models contrast agent flux in a unidirectional manner. However, contrast agent exchange is in principle bidirectional,[16] and a two-compartment bidirectional model could potentially improve the accuracy of rCBV estimates.

In the current study we aimed to determine the impact of accounting for bidirectional contrast agent exchange on rCBV estimates, as compared to unidirectional model-based rCBV estimates, and whether the association between early post-bevacizumab changes in rCBV compared to pretreatment baseline and overall survival (OS) significantly differed using the two models. We hypothesized that changes in posttreatment rCBV using the bidirectional leakage correction algorithm will better stratify GBM patients treated with bevacizumab therapy according to overall survival when compared with the unidirectional model.

Materials and Methods

Patients

All patients provided informed written consent to have their information stored in an Institutional Review Board (IRB)-approved neurooncology database for use in future investigations. Forty-seven sequential recurrent GBM (WHO grade IV) patients treated with bevacizumab who had DSC-MRI and outcome data available were retrospectively enrolled (35 men; mean age 57 years, range 28–75). Anatomic and DSC-MRI were acquired within 1 month before (4.1 ± 7.0 days; mean $\pm$ standard deviation) and 2 months (28.2 ± 11.0 days) after the start of bevacizumab therapy (10 mg/kg IV every 2 weeks).

MRI

Studies were performed at either 1.5T (Siemens Avanto or Sonata, Erlangen, Germany) or 3T (Siemens Trio, Verio, or Skyra). Precontrast standard anatomical images were acquired, including T_1-weighted, T_2-weighted, and fluid-attenuated inversion recovery (FLAIR). For DSC-MRI, a total of 0.1 mmol/kg dose of gadopentate dimeglumine (Gd-DTPA; Magnevist, Bayer Schering Pharma, Leverkusen, Germany) was administered, 0.025 mmol/kg for preload dosage to mitigate T_1-based leakage contamination[17] and the remaining 0.075 mmol/kg for dynamic bolus administration. A 2-minute gap was placed between the preload dose and the start of baseline imaging of the DSC-MRI. The range of DSC-MRI acquisition parameters included: TE/TR = 23–41/1250–1400 msec, flip angle = 35°, matrix size = 80 × 96–128 × 128, slice thickness = 4–6 mm with an interslice gap of 0–1 mm, number of slices = 6–25, number of baseline acquisitions before contrast agent injection = 10–25, and number of timepoints = 40–120. Conventional postcontrast T_1-weighted images (T_1+C) were subsequently acquired.

Image Analysis

Tumor regions of interest (ROIs) were defined by abnormal hyperintensity on T_1-weighted postcontrast images using semiautomated segmentation techniques, followed by manual inspection and adjustment of the resulting contour as described previously.[18] All DSC-MRI studies completely covered the spatial extent of contrast-enhancing tumor. DSC-MRI images were motion-corrected on the scanner and processed via in-house custom scripts in MatLab (MathWorks, Natick, MA). All simulations and calculations were performed in MatLab using custom scripts. Uncorrected rCBV was calculated using trapezoidal integration of the original DSC-MRI relaxivity–time curve, $\Delta\hat{R}_2^*(t)$. The whole-brain average relaxivity, derived from the nonenhancing voxels, was used for both the original unidirectional "Boxerman-Weisskoff" model[13] (Unidir-model) and the newly proposed bidirectional exchange model (Bidir-model). (Details regarding the Bidir-model are described in the Appendix.) Linear least-squares optimization was used to determine the free parameters for both the Bidir-model and the Unidir-model algorithms. The rCBV maps were manually registered to the corresponding posttreatment T_1+C images using *tkregister2* (Freesurfer, surfer.nmr.mgh.harvard.edu; Massachusetts General Hospital, Harvard Medical School, Cambridge, MA).

Statistical Analysis

Median rCBV was calculated from segmented tumor at baseline (pretreatment) and 6-week posttreatment timepoints for all patients. All rCBV values were normalized to median rCBV within a circular ROI drawn in the contralateral normal-appearing white matter. Histograms of rCBV were generated via GraphPad Prism 6 (La Jolla, CA) with a bin width of 0.5. We used the absolute value of percentage difference to compare the leakage correction methods because rCBV tends to increase in the presence of T_1 leakage

(between correction methods) and decrease in the presence of T_2^* leakage. The absolute difference between the two techniques was calculated as the absolute value of the difference between the two methods divided by the average of the two methods for each patient and each MRI scan.

A multivariate Cox regression model was used to determine whether pretreatment rCBV, posttreatment rCBV, change in rCBV between pre- and posttreatment timepoints, age at time of diagnosis, tumor volume, Karnofsky Performance Status (KPS), and MR field strength stratified patients according to OS. Nineteen of the 94 total pre- and posttreatment scans were acquired at 3.0T, and the remaining 75 were acquired at 1.5T, with 10 in the pretreatment group, and 9 in the posttreatment group. No significant difference, using an unpaired two-tailed *t*-test, was found between the rCBV values computed using the 3.0T scanner data and the 1.5T scanner data in either the pretreatment group ($P = 0.63$) or the posttreatment group ($P = 0.14$). Nevertheless, to guard against potential biases with regard to field strength, the pre- and posttreatment field strength as separate covariates.

Results

As described in the Appendix and as illustrated in Fig. 1, the observed DSC-MRI signal includes both the desired signal–time curve, which reflects the change in magnetic susceptibility caused by the contrast agent bolus, and the artifact caused by contrast agent extravasation. The Unidir-model (dotted blue and red curves in Fig. 1) can only fit T_1 or T_2^* leakage scenarios, where contrast agent extravasates from the intravascular space to the EES without back-flux. By comparison, the Bidir-model can fit relaxivity–time curves with a wider range of behavior. Most notably, the Bidir-model can more accurately model the late postbolus timepoints by accounting for variable rates of contrast agent backflow that can exist within different regions of a tumor and within different tumor types.

Figure 2 highlights the difference in the model fits and resulting relaxivity–time curves between the two different leakage correction algorithms in a sample tumor. The extra parameter used for the Bidir-model allows for a better fit to the raw DSC-MRI data than the Unidir-model with respect to residual errors. Both model fits can then be broken down into their respective T_1 leakage and rCBV curve components. The T_1 leakage from the Unidir-model rises almost linearly over time. On the other hand, the Bidir-model rises faster initially, but corrects the T_1 leakage curve such that the curve eventually slows down, a trend that is more reflective of what is often observed on dynamic contrast enhancing (DCE)-MRI. Whereas in the simulation the different curves arose from the same "true" rCBV curve, in experimental data the differences in leakage correction algorithms result in distinct corrected rCBV curves. Most noticeably, the primary change in rCBV comes from the first-pass curve, the difference arising from the more rapid rise in the bidirectional T_1-leakage curve. In the T_1 leakage

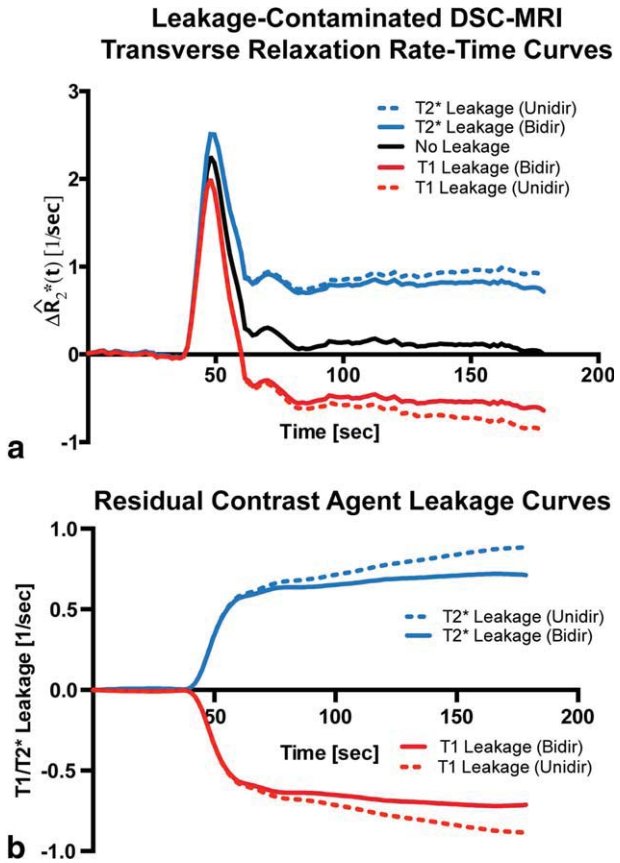

FIGURE 1: Sample simulation of DSC-MRI relaxivity–time curves. (A) The black curve reflects absence of contrast agent leakage. The blue and red curves include contrast extravasation with dominant T_2^* (overestimation of rCBV) and T_1 (underestimation of rCBV) artifact, respectively, both without (dotted) and with (dashed) inclusion of bidirectional contrast flux. The Unidir-model is limited to fitting the dotted curves (with different magnitudes), whereas the Bidir-model can fit a greater range of all leakage-contaminated curves. The raw leakage-contaminated DSC-MRI curves in (A) are a summation of the "true" relaxivity–time curve (solid black line) and the leakage contamination curves (B).

case, there is a trend of increasing rCBV from the uncorrected version to the Bidir-model.

Figure 3 illustrates a case where the mean tumor rCBV increased following bevacizumab therapy. Individual tumor rCBV values notably increased when employing more accurate leakage correction strategies, exemplified by the progressive rightward shift of the uncorrected, Unidir-model and Bidir-model rCBV histograms. The uncorrected rCBV map contained a high percentage of negative rCBV values within tumor, averaging −0.09 pretreatment and 0.29 posttreatment, highlighting the inaccuracies of uncorrected rCBV estimates. Mean tumor rCBV substantially increased when using the Unidir-model (1.72 pretreatment and 2.33 posttreatment) and increased further when using the Bidir-model (2.24 pretreatment and 2.69 posttreatment).

Next, we evaluated whether a change in rCBV from baseline to 2 months measured using the various leakage correction strategies could stratify the 47 recurrent GBM

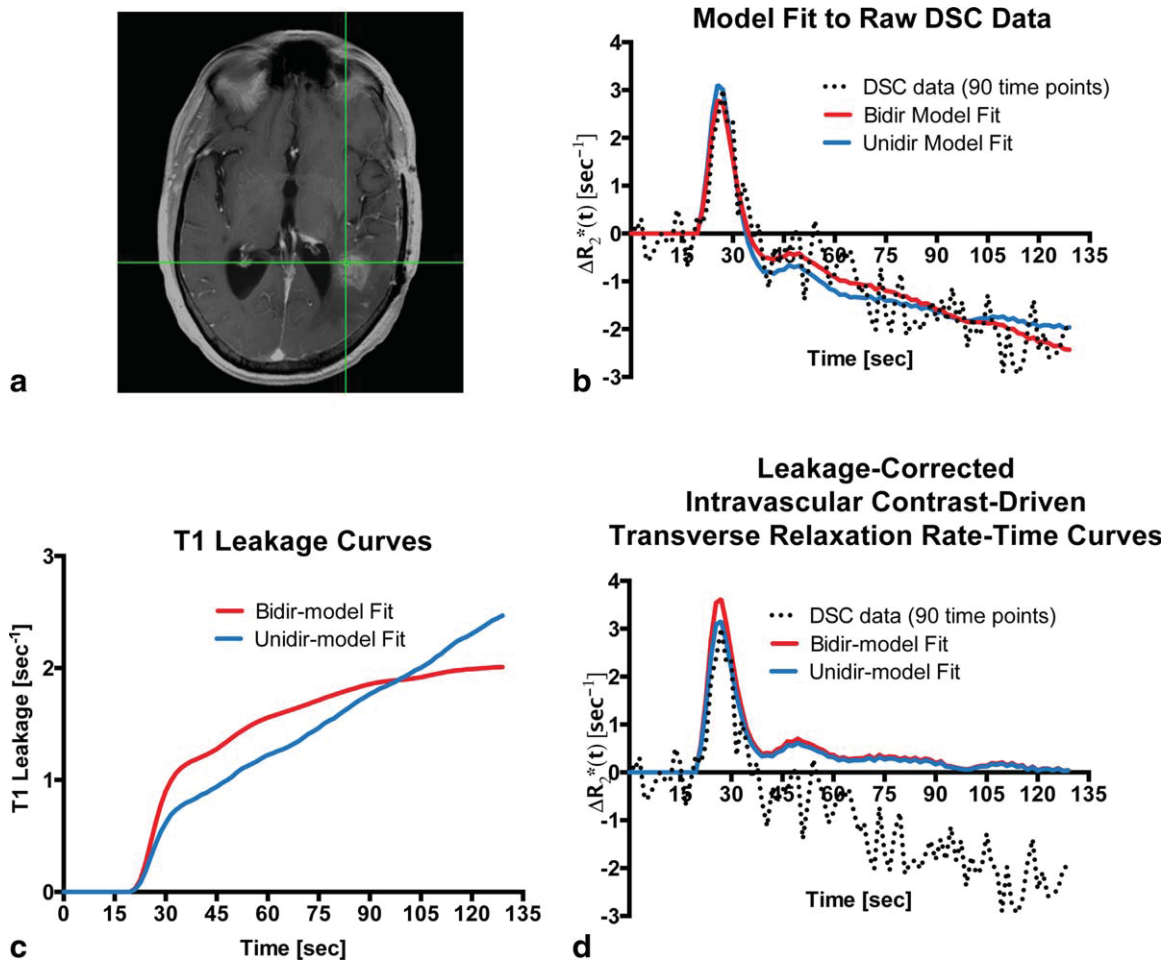

FIGURE 2: Leakage correction model comparison in tumor voxel. (A) T_1-weighted postcontrast image of a sample case of recurrent GBM and selected voxel. (B) Comparison of Bidir-model (red) and Unidir-model (blue) fits to the raw relaxivity–time data. (C) The T_1 leakage contamination curve computed with the Bidir-model is less steep than that observed with the Unidir-model and demonstrates approach towards equilibrium that is not seen on the Unidir-model curve. (D) The Bidir-model and Unidir-model corrected relaxivity–time curves differ notably in the first-pass, and both are substantially different from the raw relaxivity–time data.

patients treated with bevacizumab according to OS. In particular, we tested whether patients with decreased rCBV following bevacizumab (ΔrCBV <0) had significantly longer OS compared to patients with increased rCBV (ΔrCBV >0) after accounting for age, KPS, enhancing tumor size, and MRI field strength. Figure 4 demonstrates that both uncorrected ΔrCBV and Unidir-model ΔrCBV did not stratify patients according to OS (Cox regression; $P = 0.28$ and 0.43, respectively) in a statistically significant manner, whereas the Bidir-model ΔrCBV significantly stratified patients into long and short OS based on the change in rCBV ($P = 0.01$). Median OS for the patients whose rCBV estimated with the Bidir-model decreased following bevacizumab treatment was 358 days, versus 183 days for those with increasing rCBV. Table 1 illustrates detailed results from the Cox proportional hazards model, including effects of age, change in tumor volume, field strength at the pretreatment and posttreatment timepoints, and KPS.

The mean rCBV with the Bidir-model had a $13.9 \pm 10.3\%$ absolute difference from the Unidir-model prior to therapy and a $16.0 \pm 17.6\%$ absolute difference in rCBV after treatment over all 47 patients. Over all 94 scan sessions, there was a $14.9 \pm 14.4\%$ difference between mean leakage-corrected whole-tumor rCBV computed with the Bidir-model and Unidir-model. Interestingly, when ΔrCBV was used to characterize "responders" (ΔrCBV <0) and "nonresponders" (ΔrCBV >0), 11 of the 47 cases (23%) had different classifications using the two leakage correction algorithms. We then characterize the "responders" and "nonresponders" according to whether they had a survival time less than the median (222 days), "short-term survival," or greater than the median, "long-term survival." We considered a "correct classification" to be either a nonresponder with short-term survival or a responder with long-term survival. Among the four "nonresponders" classified by the Bidir-model, three had "short-term survival" (75%), and among the seven "responders," five had long-term survival (71%). Figure 5 illustrates one case where the bidirectional leakage correction algorithm demonstrated a decrease in rCBV in a long-term survivor, whereas the unidirectional and uncorrected rCBV did not. Posttreatment rCBV based on the uncorrected model more than doubles from pretreatment baseline, with equivalent pre- and

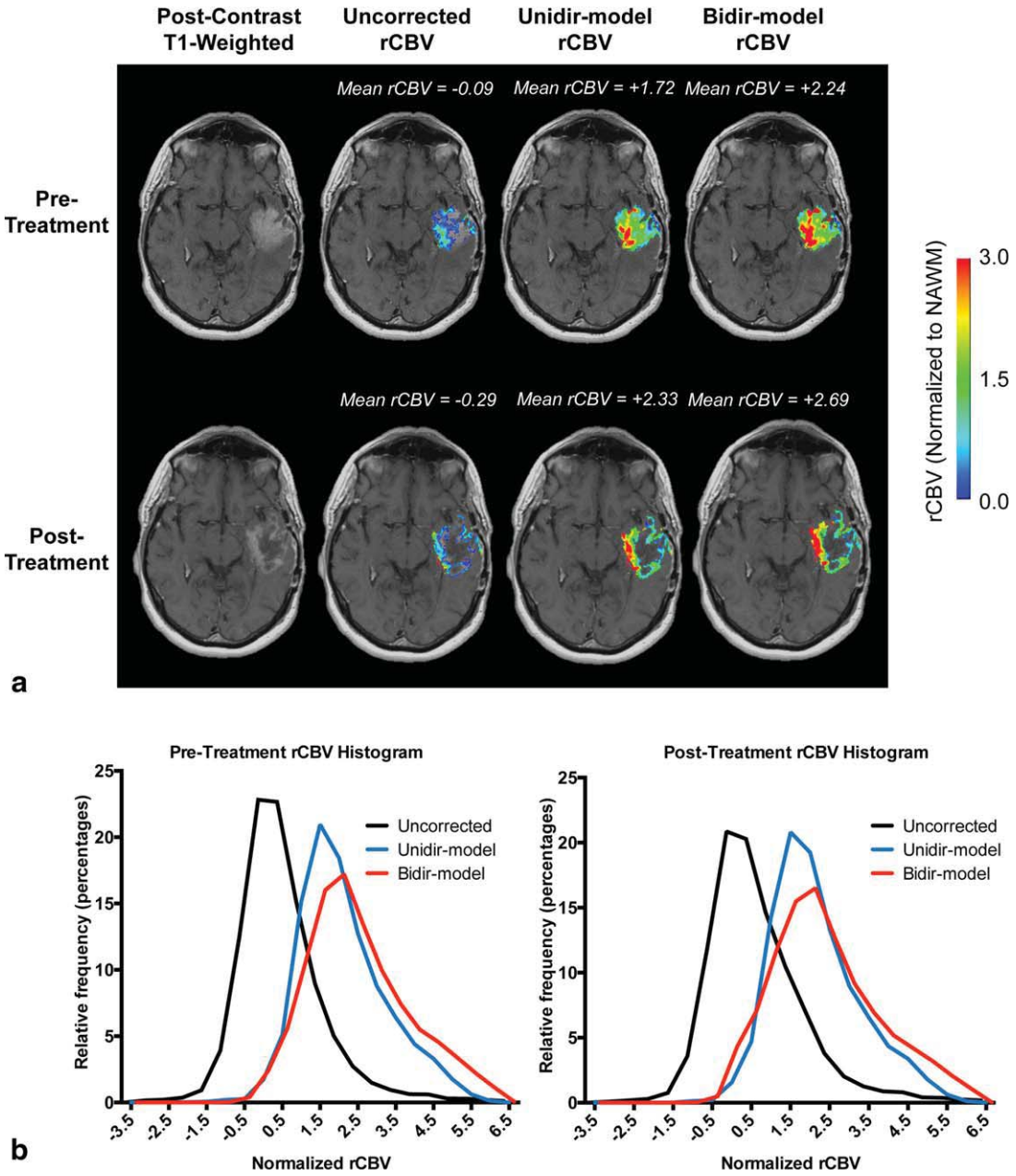

FIGURE 3: (A) Sample rCBV maps for a recurrent GBM, both pre- and post-bevacizumab treatment. Mean pre- and posttreatment tumor rCBV progressively increase when using the uncorrected, Unidir-model and Bidir-model postprocessing strategies. (B) There is a progressive rightward shift of the uncorrected, Unidir-model and Bidir-model rCBV histograms, demonstrating that the increase in mean rCBV is due to increased rCBV in the entire population of voxels, not just a few, as expected in a T_1-leakage scenario.

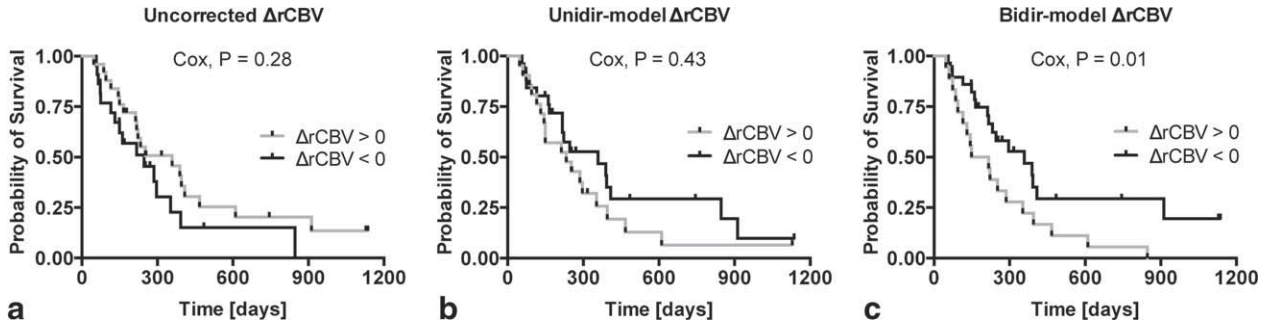

FIGURE 4: Kaplan–Meier survival plots for ΔrCBV, with patients stratified according to whether rCBV increased or decreased using (A) uncorrected rCBV, (B) Unidir-model rCBV, and (C) Bidir-model rCBV.

TABLE 1.

Variable	*Hazard Ratio*	*Standard Error*	*p-value*	*95% C.I.*
ΔrCBV > 0 *(Uncorrected)*	0.64	0.41	0.28	0.29, 1.42
Age at recurrence	1.02	0.02	0.25	0.98, 1.06
Change in tumor volume	1.00	0.01	0.98	0.97, 1.03
Field Strength (Pre-tx)	0.65	0.33	0.19	0.34, 1.24
Field Strength (Post-tx)	1.97	0.57	0.24	0.64, 3.02
KPS	0.99	0.02	0.41	0.95, 1.02
ΔrCBV > 0 *(Unidirectional)*	1.33	0.36	0.43	0.66, 2.67
Age at recurrence	1.02	0.02	0.28	0.98, 1.06
Change in tumor volume	1.00	0.01	0.79	0.98, 1.03
Field Strength (Pre-tx)	0.68	0.34	0.25	0.35, 1.31
Field Strength (Post-tx)	1.66	0.36	0.16	0.82,3.34
KPS	0.99	0.02	0.55	0.95, 1.03
ΔrCBV > 0 *(Bidirectional)*	3.12	0.42	**0.01***	1.37,7.10
Age at recurrence	1.01	0.02	0.65	0.97, 1.05
Change in tumor volume	0.99	0.01	0.64	0.97, 1.02
Field Strength (Pre-tx)	0.67	0.34	0.36	0.35, 1.30
Field Strength (Post-tx)	2.43	0.38	0.02	1.14,5.18
KPS	0.98	0.02	0.36	0.95, 1.02

posttreatment rCBV using the Unidir-model. However, the Bidir-model yields a substantial decrease from pretreatment to posttreatment rCBV, which is concordant with the long OS in this patient (1149 days). The rightward shifts of the rCBV histograms illustrate that differences in mean tumor rCBV are not merely reflecting a large change for few voxels, but rather a global change over the entire tumor.

Discussion

The results from this study support the hypothesis that DSC-MRI leakage correction accounting for bidirectional contrast agent exchange may yield significantly different estimates of tumor rCBV compared with the standard "Boxerman-Weisskoff" unidirectional model and the uncorrected model. We found that early changes in rCBV estimated using the Bidir-model better stratify bevacizumab-treated recurrent GBM patients according to OS as compared to estimates using the Unidir-model. In accordance with the notion that efficacious therapy works by reducing tumor vascularity, this supports the hypothesis that bidirectional contrast agent exchange using a two-compartment model similar to DCE-MRI more accurately represents contrast agent pharmacokinetics within tumor vasculature.

In this study the direction of change from baseline in rCBV using the Bidir-model stratified patients according to OS. However, in contrast to recent studies by Schmainda et al[19] and Kickingereder et al,[20] using absolute measures of pre- and posttreatment rCBV did not achieve statistical significance. This could potentially be attributed to differences in methodology, as the current study normalized rCBV to the contralateral, normal-appearing white matter. By comparison, Schmainda et al[19] used a standardized rCBV, where the white matter is controlled to be within a certain range of intensities, and Kickingereder et al[20] normalized rCBV by the arterial input function using a *k*-means cluster algorithm.

When introduced, the standard Unidir-model significantly improved rCBV estimates compared to those made without leakage correction.[13] The addition of a preload or incubation dose to Unidir-model postprocessing leakage correction further reduced T_1-leakage effects by increasing EES contrast agent concentration prior to dynamic bolus injection, yielding greater improvement in rCBV measurements obtained without leakage correction.[14,21] However, the lack of a contrast agent backflow term may lead to an incomplete elimination of the T_1 or T_2^* leakage artifact, especially in the presence of a preload because the total contrast agent concentration in the EES is no longer negligible (which ensures the concentration gradient is purely unidirectional), even with short DSC-MRI acquisition times. This is likely a factor contributing to the observed 14.9% difference in

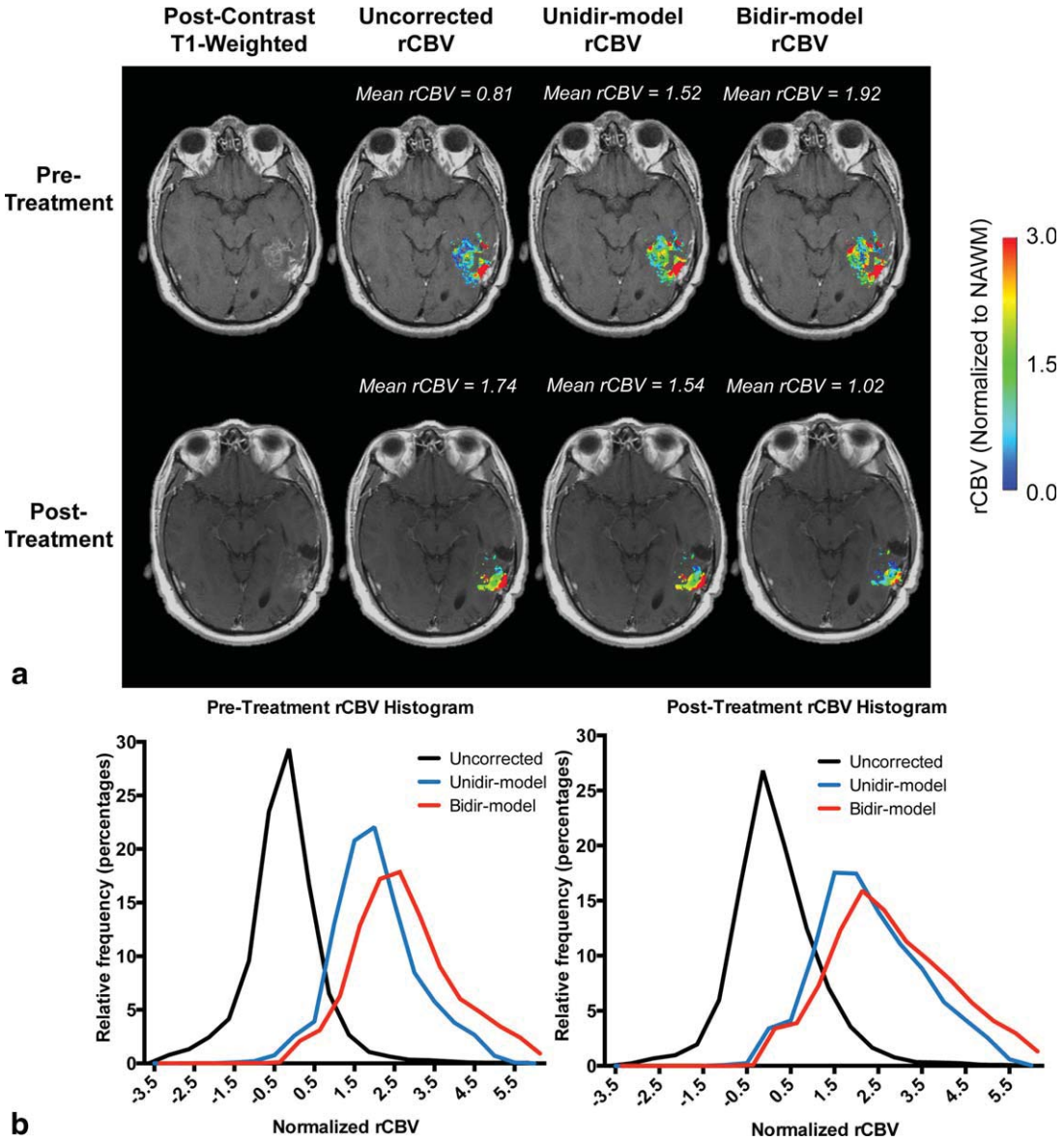

FIGURE 5: (A) Comparison of rCBV maps of recurrent GBM based on uncorrected, Unidir-model, and Bidir-model methodologies in a patient with long-term survival (1149 days). Whereas the Bidir-model demonstrates a substantial decrease in rCBV posttreatment, in accordance with favorable OS, the uncorrected and Unidir-model estimates of increasing or stable rCBV misclassify the patient as having poor prognosis. (B) rCBV histograms demonstrate a rightward shift of the Uncorrected and Unidir-model in the post-treatment setting as compared to the pre-treatment setting, whereas the Bidir-model had a leftward shift, demonstrating global rCBV changes in opposite directions after treatment rather than in just a few voxels.

rCBV between the different leakage correction algorithms, since we used a preload in the current study. It is important to note that this magnitude of difference in rCBV between the Bidir-model and Unidir-model may be clinically meaningful and could potentially impact clinical decision-making.

This study has certain notable limitations. First, the DSC-MRI protocols had variable TEs and TRs, with a varying number of slices, slice thicknesses, and field strengths. Although this permitted generalization of our results across a variety of acquisition schemes and MRI platforms, it is unclear whether the same magnitude of differences between the leakage correction algorithms would be maintained in a trial with a single standardized acquisition protocol. Additionally, the time between the MR scans and treatments varied slightly between patients, which may have reduced our ability to assess treatment response. In a clinical trial, these would ideally be more standardized throughout the patient cohort. Given the relatively small sample size and retrospective nature, which includes biases inherent to such retrospective studies, this investigation was exploratory and larger studies are needed to evaluate the potential impact of the leakage correction algorithms on clinical decision-making. Furthermore, a scanning protocol might be useful to develop in order to provide a more standardized approach for DSC-MRI, even for clinical use in the future.

Furthermore, this study assumes the use of a gadolinium-based contrast agent, which often leaks into the extravascular space when vascular permeability is disrupted.

Currently, pure intravascular contrast agents, such as ferumoxytol, are not approved for central nervous system (CNS) imaging, although it is approved for MR angiography. The main advantage of using intravascular contrast agents for perfusion imaging is the lack of extravasation into the extravascular space, eliminating the need for leakage correction algorithms or preload injection.[22] On the other hand, because it is a blood pool agent, the enhancement pattern of biological tissues may differ as compared with gadolinium-based contrast agents, with the possibility of susceptibility artifacts arising.[23] Furthermore, there is potentially a requirement of 2 consecutive days of imaging to obtain relatively intracellular-weighted or interstitial-weighted images, the scans that would be more analogous to the gadolinium-based anatomical scans.[24]

The use of a bidirectional leakage correction model changed the estimated rCBV values significantly compared to both the standard unidirectional leakage correction model and rCBV measured without leakage correction, despite relatively short DSC-MRI acquisition times. The change from pretreatment baseline in rCBV estimated using the Bidir-model 2 months after bevacizumab therapy in recurrent GBM stratified patients according OS, whereas uncorrected and standard Unidir-model estimates of change in rCBV did not.

Appendix

Following eq. A6 of Boxerman et al.,[13] the leakage-contaminated DSC-MRI relaxation rate–time curve, $\Delta\hat{R}_2^*(t)$ equals intravascular contrast-driven transverse relaxation rate change, $\Delta R_2^*(t)$, plus $\Delta R_{2,E}^*(t)$, a tissue leakage term describing the simultaneous T_1 and T_2^* relaxation effects resulting from gadolinium extravasation:

$$\Delta\hat{R}_2^*(t)=\Delta R_2^*(t)+\Delta R_{2,E}^*(t)=\Delta R_2^*(t)+\left[r_{2,E}^*-\frac{TR}{TE}\cdot\left(\frac{E_1}{1-E_1}\right)\cdot r_1\right]C_E(t) \quad (1)$$

where $E_1=e^{-TR/T_{1o}}$, T_{1o} is the precontrast tissue T_1, r_1 is the T_1 relaxivity of gadolinium, $C_E(t)$ is the concentration of gadolinium in the extravascular, extracellular space, and $r_{2,E}^*$r represents the T_2^* relaxation effects of gadolinium extravasation, as described by Quarles et al[25] and Schmiedeskamp et al.[26] From the original Tofts model describing bidirectional contrast agent flux between the intravascular and extravascular compartments[16]:

$$C_E(t)=k_{trans}\cdot\left(C_p(t)*e^{-k_{ep}t}\right) \quad (2)$$

where k_{trans} and k_{ep} are the transfer coefficients for intra- to extravascular and extra- to intravascular contrast flux, respectively, and $C_p(t)$ is the plasma contrast concentration. $C_p(t)$ and $\Delta R_2^*(t)$ can be defined as scaled versions of the whole-brain average relaxation rate in nonenhancing voxels, $\Delta\bar{R}_2^*(t)$[13]:

$$C_p(t)=k\cdot\Delta\bar{R}_2^*(t) \quad (3)$$

$$\Delta R_2^*(t)=K_1\cdot\Delta\bar{R}_2^*(t) \quad (4)$$

Combining Eqs. (1)–4 yields:

$$\Delta\hat{R}_2^*(t)=K_1\cdot\Delta\bar{R}_2^*(t)-K_2\int_0^t\Delta\bar{R}_2^*(\tau)\cdot e^{-k_{ep}(t-\tau)}d\tau \quad (5)$$

where

$$K_2=\left[r_{2,E}^*-\frac{TR}{TE}\cdot\left(\frac{E_1}{1-E_1}\right)\cdot r_1\right]\cdot k_{trans}\cdot k \quad (6)$$

K_1, K_2, and k_{ep} (units of sec^{-1}) are the free parameters of Eq. (5). In general, K_1 depends on CBV, vessel size, and other physiologic factors, while K_2 is related to vascular permeability. Substituting $k_{ep}=0$, which occurs with no backflow of extravasated contrast agent, yields the original Weisskoff-Boxerman leakage correction algorithm, where K_1 and K_2 are solved by linear least-squares fit to $\Delta\hat{R}_2^*(t)$.[13] For the Bidir-model correction method, a linear least-squares fit to K_1, K_2, and k_{ep} can be employed using the methodology of Murase,[27] as described by the following equation:

$$\Delta\hat{R}_2^*(t)=(K_2+k_{ep}\cdot K_1)\int_0^{t_k}\Delta\hat{R}_2^*(\tau)\,d\tau-k_{ep}\cdot\int_0^{t_k}\Delta\hat{R}_2^*(\tau)\,d\tau+K_1\cdot\Delta\hat{R}_2^*(t) \quad (7)$$

Integrating the corrected relaxation rate-time curve yields leakage-corrected rCBV:

$$rCBV_{corr}=rCBV+K_2\int_0^T\int_0^t\Delta\hat{R}_2^*(\tau)\cdot e^{-k_{ep}(t-\tau)}d\tau dt \quad (8)$$

Acknowledgments

Contract grant sponsor: American Cancer Society (ACS); contract grant number: Research Scholar Grant RSG-15-003-01-CCE (to B.M.E.); Contract grant sponsor: National Brain Tumor Society Research Grant (to B.M.E.); Contract grant sponsor: Art of the Brain (to T.F.C.); Contract grant sponsor: Ziering Family Foundation in memory of Sigi Ziering (to T.F.C.); Contract grant sponsor: Singleton Family Foundation (to T.F.C.); Contract grant sponsor: Clarance Klein Fund for Neuro-Oncology (to T.F.C.); Contract grant sponsor: National Institute of Health National Institute of General Medical Sciences; contract grant number: GM08042 (to K.L.); Contract grant sponsor: University of California Los Angeles Medical Scientist Training Program (to K.L.).

We thank our research coordinators, Fady Mansour and Polly Kay, our research MR technologists Sergio Godinez, Glen Nyborg, Francine Cobla, and Kelly O'Connor, the

nurses and nurse assistants, and Adrian Ibarra in the Department of Neurosurgery for their assistance in coordinating and running the patient studies, as well as the patients and their families for volunteering for our research.

References

1. Ostrom QT, Gittleman H, Fulop J, et al. CBTRUS statistical report: primary brain and central nervous system tumors diagnosed in the United States in 2008-2012. Neurooncology 2015;17(Suppl 4):iv1–iv62.
2. Ostrom QT, Gittleman H, Liao P, et al. CBTRUS statistical report: primary brain and central nervous system tumors diagnosed in the United States in 2007-2011. Neurooncology 2014;16(Suppl 4):iv1–63.
3. Johnson DR, O'Neill BP. Glioblastoma survival in the United States before and during the temozolomide era. J Neurooncol 2012;107:359–364.
4. Brem S, Cotran R, Folkman J. Tumor angiogenesis: a quantitative method for histologic grading. J Natl Cancer Inst 1972;48:347–356.
5. Wen PY, Macdonald DR, Reardon DA, et al. Updated response assessment criteria for high-grade gliomas: response assessment in neuro-oncology working group. J Clin Oncol 2010;28:1963–1972.
6. Nowosielski M, Wiestler B, Goebel G, et al. Progression types after antiangiogenic therapy are related to outcome in recurrent glioblastoma. Neurology 2014;82:1684–1692.
7. LaViolette PS, Cohen AD, Prah MA, et al. Vascular change measured with independent component analysis of dynamic susceptibility contrast MRI predicts bevacizumab response in high-grade glioma. Neuroncology 2013;15:442–450.
8. Leu K, Enzmann D, Woodworth D, et al. Hypervascular volume estimated by comparison to a large-scale cerebral blood volume (Cbv) radiographic atlas predicts survival in recurrent glioblastoma treated with bevacizumab. Neurooncology 2014;16.
9. Harris RJ, Cloughesy TF, Hardy AJ, et al. MRI perfusion measurements calculated using advanced deconvolution techniques predict survival in recurrent glioblastoma treated with bevacizumab. J Neurooncol 2015;122:497–505.
10. Meier P, Zierler KL. On the theory of the indicator-dilution method for measurement of blood flow and volume. J Appl Physiol 1954;6:731–744.
11. Essig M, Nguyen TB, Shiroishi MS, et al. Perfusion MRI: the five most frequently asked clinical questions. AJR Am J Roentgenol 2013;201: W495–510.
12. Rosen BR, Belliveau JW, Vevea JM, Brady TJ. Perfusion imaging with NMR contrast agents. Magn Reson Med 1990;14:249–265.
13. Boxerman JL, Schmainda KM, Weisskoff RM. Relative cerebral blood volume maps corrected for contrast agent extravasation significantly correlate with glioma tumor grade, whereas uncorrected maps do not. AJNR Am J Neuroradiol 2006;27:859–867.
14. Paulson ES, Schmainda KM. Comparison of dynamic susceptibility-weighted contrast-enhanced MR methods: recommendations for measuring relative cerebral blood volume in brain tumors. Radiology 2008;249:601–613.
15. Weisskoff R, Boxerman JL, Sorenson AG, Kulke STC, Rosen BR. Simultaneous blood volume and permeability mapping using a single Gd-based contrast injection. In: Proc 2nd Annual Meeting ISMRM, San Francisco; 1994.
16. Tofts PS, Kermode AG. Measurement of the blood-brain barrier permeability and leakage space using dynamic MR imaging. 1. Fundamental concepts. Magn Reson Med 1991;17:357–367.
17. Schmainda KM, Rand SD, Joseph AM, et al. Characterization of a first-pass gradient-echo spin-echo method to predict brain tumor grade and angiogenesis. AJNR Am J Neuroradiol 2004;25:1524–1532.
18. Ellingson BM, Cloughesy TF, Lai A, Nghiemphu PL, Mischel PS, Pope WB. Quantitative volumetric analysis of conventional MRI response in recurrent glioblastoma treated with bevacizumab. Neurooncology 2011;13:401–409.
19. Schmainda KM, Zhang Z, Prah M, et al. Dynamic susceptibility contrast MRI measures of relative cerebral blood volume as a prognostic marker for overall survival in recurrent glioblastoma: results from the ACRIN 6677/RTOG 0625 multicenter trial. Neurooncology 2015 [Epub ahead of print].
20. Kickingereder P, Wiestler B, Burth S, et al. Relative cerebral blood volume is a potential predictive imaging biomarker of bevacizumab efficacy in recurrent glioblastoma. Neurooncology 2015;17:1139–1147.
21. Hu LS, Baxter LC, Pinnaduwage DS, et al. Optimized preload leakage-correction methods to improve the diagnostic accuracy of dynamic susceptibility-weighted contrast-enhanced perfusion MR imaging in posttreatment gliomas. AJNR Am J Neuroradiol 2010;31:40–48.
22. Gahramanov S, Muldoon LL, Li X, Neuwelt EA. Improved perfusion MR imaging assessment of intracerebral tumor blood volume and antiangiogenic therapy efficacy in a rat model with ferumoxytol. Radiology 2011;261:796–804.
23. Fananapazir G, Marin D, Suhocki PV, Kim CY, Bashir MR. Vascular artifact mimicking thrombosis on MR imaging using ferumoxytol as a contrast agent in abdominal vascular assessment. J Vasc Interv Radiol 2014;25:969–976.
24. Farrell BT, Hamilton BE, Dosa E, et al. Using iron oxide nanoparticles to diagnose CNS inflammatory diseases and PCNSL. Neurology 2013; 81:256–263.
25. Quarles CC, Gochberg DF, Gore JC, Yankeelov TE. A theoretical framework to model DSC-MRI data acquired in the presence of contrast agent extravasation. Phys Med Biol 2009;54:5749–5766.
26. Schmiedeskamp H, Andre JB, Straka M, et al. Simultaneous perfusion and permeability measurements using combined spin- and gradient-echo MRI. J Cereb Blood Flow Metab 2013;33:732–743.
27. Murase K. Efficient method for calculating kinetic parameters using T-1-weighted dynamic contrast-enhanced magnetic resonance imaging. Magn Reson Med 2004;51:858–862.